An Investigation of Plasma Parameters of a High-Current Hollow-Cathode Glow Discharge[1]

I.A. Shemyakin, A.V. Bolotov, Yu.D. Korolev, N.V. Landl, O.B. Frants, and J. Urban*

Institute of High Current Electronics SB RAS, 2/3, Academichesky ave., Tomsk, 634055, Russia
Phone: 8(3822) 49-13-97, Fax: 8(3822) 49-24-10, E-mail: shemyakin@lnp.hcei.tsc.rul
**University of Erlangen-Nurenberg, 1, Erwin-Rommel-St, Erlangen, D-91058, Germany*

Abstract – The paper presents the results of measurements of the plasma parameters of a pseudospark discharge operating in hydrogen. Most of the experimental data were obtained by high temporal and spatial resolution spectroscopy of the radiation intensity in different discharge regions. Peculiar attention was given to the stage of superdense glow discharge. The setup and the methods of measurements used in the work are described. The behavior of spectral lines in different discharge regions is considered. A new method of measuring the electron temperature is proposed. The results of measurements of the electron temperature and electron density at different discharge stages are presented and the mechanism of energy delivery to the negative plasma column region is discussed.

1. Introduction

Recently, considerable interest has been shown in facilities with a moderate energy in a single pulse and a high pulse repetition rate for extreme ultraviolet (EUV) lithography at a wavelength of ~ 13.5 nm. One of the latest approaches to the EUV production is based on a pseudospark electrode system or more precisely, on a high-current hollow-cathode discharge [1]. Traditionally, the mechanism of the EUV generation from a pseudospark discharge rests on the concept of magnetic field compression of the plasma column [2, 3]. However, recent studies show that some experimental facts do not fit into the above concept [4]. An alternative concept uses the idea that the increase in electron density in the plasma column is governed by heavy particle ionization of both thermal and high-energy electrons taken off the cathode surface and accelerated in the cathode layer [5]. It is supposed that thermal electrons play a decisive role in energy transfer and that the electron temperature T_e must be no less then 8 eV.

This paper presents the results of measurements of the plasma parameters, such as the electron density and the electron temperature, at different discharge stages with high temporal and spatial resolution. A new method is proposed for measuring the electron temperature in the nonequilibrium plasma of a low-pressure gas discharge. It is shown that at the stage of superdense glow discharge, metal vapor of the cathode material appears in the discharge plasma column. It is concluded that the vapor results in numerous microexplosions on the cathode surface. The electron density in the discharge plasma column $n_e \approx 5 \cdot 10^{14}$–$10^{16}$ cm^{-3} and the electron temperature T_e = 1–1.1 eV. It is thought that energy is transferred mainly by fast electrons.

2. Experimental setup and measurement procedure

Figure 1 shows schematic of the chamber in which a discharge is ignited. The main gap d between cathode *1* and anode *2* was 4 mm. The diameter of the cathode aperture d_c = 3 mm and that of the anode aperture d_a = 5 mm. The main electrodes were made of copper. In the experiments, a low-pressure discharge was initiated in hydrogen at the pressure $p \approx$ (15–45) Pa. The main capacitance C_0 = 1.25 μF. The circuit impedance was ~ 0.5 Ω. The initial voltage across the gap V_0 was about (1–3) kV. In these conditions, the maximum current approximated 1.5 kA. The breakdown in the chamber was static.

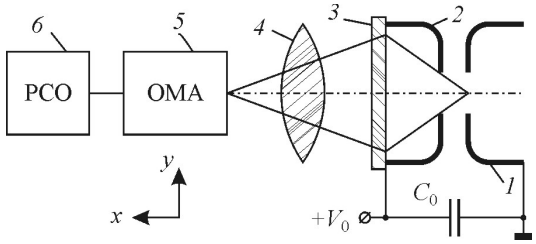

Fig. 1. Experimental setup: *1* – cathode; *2* – anode; *3* – quartz window; *4* – lens; *5* – optical multichannel analyzer; *6* – registration adaptor

Figure 1 also shows a system with temporal and spatial resolution for measuring the plasma parameters. The optical axis was directed along the X-axis. Lens *4* ensured a sharp reflection of the plasma image to the entrance slit of optical multichannel analyzer *5*. Spatial scanning was realized by shifting the lens *4* perpendicular to the optical axis in the *Y* direction. The main characteristics of the optical system were the material (quartz or glass), the focal distance f = (100–200) nm, and the lens diameter D_l = 40 mm.

[1] The work was supported by the Russian Foundation for Basic Research (Project No. 08-02-00912-a).

The spectral range was 300–830 nm. The temporal and spatial resolutions $\Delta t = 2$ ns and $\Delta y = 0.2$ mm, respectively. In the experiments, we investigated the emission from the center of the cathode hole (the discharge column) and near the cathode edge (cathode-spot emission, cathode flare, and partial-discharge column).

3. Measurement of the plasma parameters

In the experiments, the parameters to be measured were the electron temperature T_e and the electron density n_e. The electron density was measured from H_α and H_β Balmer series lines profiles. For measuring the electron temperature, we used the method of relative ion-to-atom intensity of copper spectral lines appearing in the emission spectra. Let us dwell on this method, as applied to our experiments.

Group methods based on the relative intensity of spectral lines have two main shortcomings: low accuracy and narrow applicability. Actually, for attaining a reasonably high accuracy, the difference between excitation energy of spectral lines ΔE must be not less than 15–20 eV [6]. As for the second problem, the method is applicable only within the model of local thermodynamic equilibrium (LTE), which is normally unattainable in low-temperature plasmas. Therefore, one should take into account that the temperature estimated by this method (so-called distribution temperature T_p) is lower than the actual temperature T_e. Generally, the higher the deviation from equilibrium conditions, the larger the difference between T_p and T_e. At the same time, it can be assumed that under certain conditions, this deviation is negligibly small and the method turns out to be well applicable even if the plasma is not in strictly equilibrium conditions. We will analyze this problem below and present a relation between T_p and T_e that allows this conclusion in our experimental conditions.

Figure 2 shows a block diagram typical of our experimental conditions. Energy level (1) of Cu atoms is characterized by the n_1 population and by the excitation energy E_1. This level is not in equilibrium with the ground state of an atom, but it is in equilibrium with the ground state of the first ion. The block (group) 4s is also in equilibrium with the ground state of the first ion.

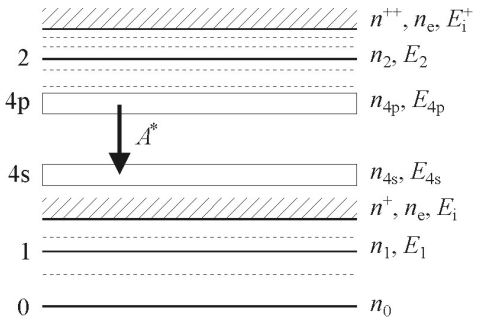

Fig. 2. Block diagram of the energy levels of CuI and CuII

The block of levels 4p features a reduced population corresponding to equilibrium due to intense radiation (with characteristic effective A^*), i.e., the levels 4p and 4s are not in equilibrium. The levels higher than 4p are also in equilibrium between each other. For the levels 4p and 4s, let us introduce the parameter δ characterizing the deviation from equilibrium conditions:

$$\delta = \frac{A^*}{k_{4p,4s} n_e}, \qquad (1)$$

where $k_{4p,4s}$ is the effective constant for de-excitation of the block 4p due to superelastic collisions. It is seen that for $\delta << 1$ we have equilibrium, otherwise have not.

Let us derive a relation between the population of the ion level (2) and the atom level (1). The populations of the block 4s and of the level (1) are related by the Saha and Boltzmann equations:

$$\frac{n_{4s}}{n_1} = 6.04 \cdot 10^{21} \frac{1}{n_e} \frac{g_{4s}}{g_1} T_e^{3/2} \exp\left(-\frac{\Delta E_{4s,1}}{T_e}\right), \qquad (2)$$

where $\Delta E_{4s,1}$ is the energy interval between the block 4s and the level (1), g_{4s} and g_1 are the total statistical weights for the block 4s and level (1), and T_e is the electron temperature in energy units.

The relation between the population of the block 4p and the level (1) is derived using the expression obtained earlier:

$$\frac{n_{4p}}{n_{4s}} = \frac{g_{4p}}{g_{4s}} \exp\left(-\frac{\Delta E_{4p,4s}}{T_e}\right)\left(\frac{1}{1+\delta}\right), \qquad (3)$$

where $\Delta E_{4p,4s}$ is the energy interval between the blocks 4s and 4s.

Substituting n_{4s} from (3) to (2) and taking into account the Boltzmann's equation for the block 4p and the level (2) gives us the equation relating the population of the levels (1) and (2):

$$\frac{n_2}{n_1} = 6.04 \cdot 10^{21} \frac{1}{n_e} \frac{g_2}{g_1} T_e^{3/2} \exp\left(-\frac{\Delta E_{2,1}}{T_e}\right)\left(\frac{1}{1+\delta}\right), \qquad (4)$$

where g_2 is the statistical weight for the level (2) and $\Delta E_{2,1}$ is the energy interval between the levels (1) and (2).

On the other hand, reasoning from the definition for T_p, we can write:

$$\frac{n_2}{n_1} = 6.04 \cdot 10^{21} \frac{1}{n_e} \frac{g_2}{g_1} T_p^{3/2} \exp\left(-\frac{\Delta E_{2,1}}{T_p}\right). \qquad (5)$$

By equating the right sides of Eqs. (4) and (5), we obtain a transcendent equation for T_p and T_e:

$$\frac{3}{2} \ln\left(\frac{T_p}{T_e}\right) = \frac{\Delta E_{2,1}\left(T_e - T_p\right)}{T_e T_p} + \ln\left(\frac{1}{1+\delta}\right). \qquad (6)$$

This equation has an analytical solution. In particular, the Maple computer code gives us this solution in the form

$$T_p = T_e\left(3LambertW \cdot FT_e - 2\Delta E_{2,1} - 2\ln(1+\delta)T_e\right), \quad (7)$$

where $F = F(T_e, \Delta E_{2,1}, \delta)$.

Equation (7) allows us to obtain the dependence $T_e = f(T_p, \Delta E_{2,1}, \delta)$ so that knowing T_p, we can calculate T_e. However, these calculations require quantitative data for the parameter δ.

The δ parameter was calculated for $T_e = 1$–8 eV and $n_e = 10^{15}$–10^{16} cm^{-3} using the diffusion approximation method [7].

It was obtained that for the electron density $n_e \le 5 \cdot 10^{15}$ cm^{-3}, $\delta \ge 1$, i.e., the plasma is in nonequilibrium conditions.

Knowing the measured values of T_p and n_e, equation (7) allows calculation of the electron temperature T_e. Example of the calculation is shown in Fig. 3. The calculations have been made for $\Delta E_{2,1} = 20$ eV.

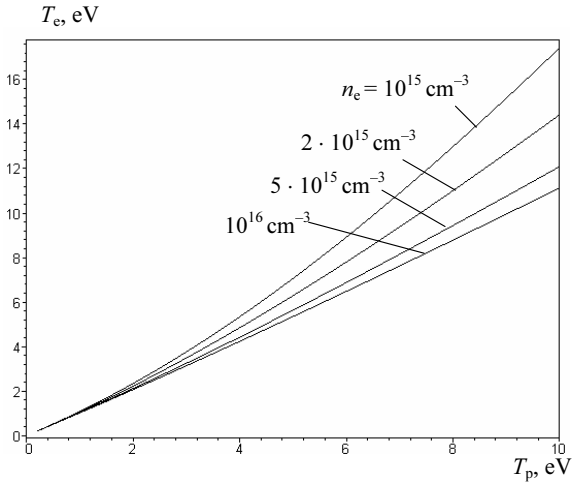

Fig. 3. Relation between T_p and T_e for different electron densities n_e

Note that for $n_e \ge 5 \cdot 10^{15}$ cm^{-3}, the decrease in T_p relative to T_e is slight (about 10%). This is comparable to the accuracy of measurements. For lower electron densities, we can refine the measured value of T_e using the data shown in Fig. 3.

4. Results and discussion

In the spectrum of the pseudospark discharge plasma, lines of neutral atoms, first and second Cu ions, and H_α and H_β Ballmer series lines are observed. Fig. 4 shows time resolved emission of Cu lines for different discharge regions and oscillograms of the voltage and current. The initial voltage $V_0 = 1200$ V and the pressure $p = 45$ Pa. The characteristic time points are indicated by arrows. Before discussing the behavior of the line intensity, let us consider the obtained plasma parameters.

Table I presents data on the electron density for different time points and discharge regions. It is seen that in the discharge column, the electron density $n_e = 5 \cdot 10^{14}$–$8 \cdot 10^{15}$ cm^{-3} and near the cathode edge, $n_e \approx 5 \cdot 10^{16}$ cm^{-3}.

Table I

Time points		1	2	3	4
n_e 10^{15}, cm^{-3}	column	0.5	3	8	10
	cathode edge				50

Table II shows the electron temperature T_e for different discharge stages and discharge regions. The electron temperature was measured using CuI (515.32 nm), CuI (521.82 nm), CuII (490.97 nm), and CuII (493.16 nm) lines. The temperature T_e was refined using equations (7). It can be seen that in the discharge column, the electron temperature $T_e = 1.0$–1.1 eV and near the cathode edge, $T_e = 0.6$–0.8 eV.

Table II

Time points		1	2	3
T_e, eV	column	0.5	3	8
	cathode edge		0.6	0.8

Let us attempt to identify the stages of the discharge operation using both the plasma parameters experimental data and the data presented in the Fig. 4, *a*.

Within the time interval between points *1* and *2*, there are no emissions of neutral atoms, first and second ions. The discharge voltage is ~ 700 V. We can say that the discharge in this case is in the dense glow stage. At interval *2–3*, emission of neutral atoms and first ions occurs. The discharge voltage is ~ 600 V and the electron temperature $T_e = 0.6$ eV. In this case, no cathode spot of the second type and arc is found, since the voltage is high and the temperature is low. However, there are numerous micro-explosions at the cathode surface. This stage is the superdense glow discharge stage. At point 4, the emissions intensity of neutral atoms and first ions decreases and that of second ions increases, and the electron density becomes higher. Hence, we have the early stage of the arc. Now let us turn to the emission from the discharge column (Fig. 4, *b*).

At the dense glow discharge stage (points *1–2*), no emissions of neutral atoms, first and second ions occurs. At the superdense glow discharge stage (points *2–3*), emission of neutral atoms and first ions arises. Interestingly, the emission intensity for the first ions is higher than that for the neutral atoms and the emissions of the second ions is absent. This fact can be explained taking into account that the electron temperature is ~ 1 eV. Actually, under these conditions, the ion fraction of the plasma is determined mainly by the first ions. At the point in time *4*, the emission intensity of the first ions decreases and that of the second ions increases. Apparently, this is due to the

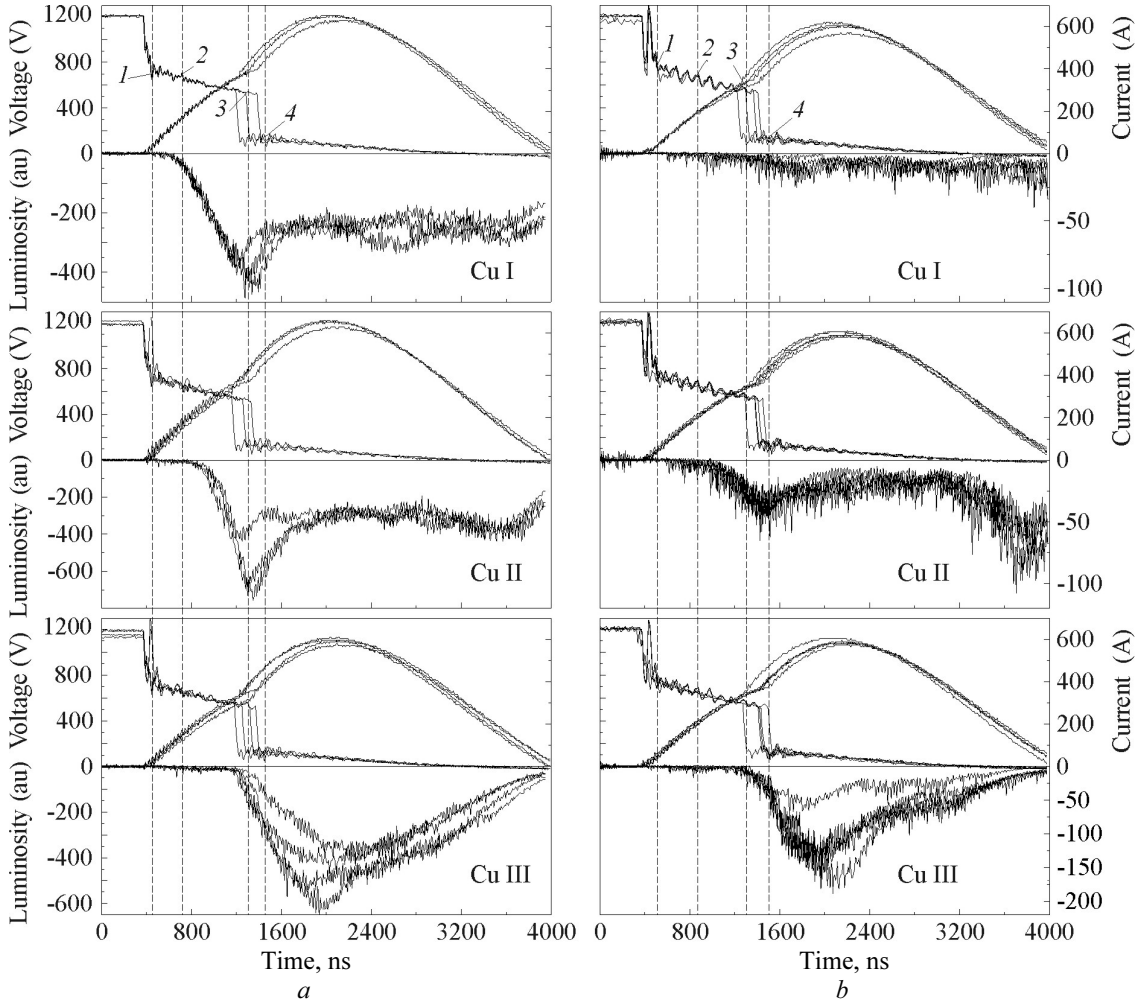

Fig. 4. Time resolved Cu lines for different discharge regions and oscillograms of the voltage and current: *a* – near the cathode edge region; *b* – discharge column. CuI, λ = 515.32 nm; CuII, λ = 491.16 nm; CuIII, λ = 435.19 nm

increase in electron temperature during the glow-to-arc transition; the second ions dominate in the plasma.

Accurate measurements of the thermal electron temperature in the plasma column of the superdense glow discharge give $T_e \approx 1$ eV. This is contradictory to the conclusion made in [5] that the thermal electrons play a leading part in the energy transfer. Evidently, the fast electrons accelerated in the cathode layer make the major contribution to the process.

References

[1] Yu.D. Korolev, O.B. Frants, N.V. Landl et al., Russian Physics J. **11**, Appendix, 169 (2006).

[2] K. Bergmann, G. Schriever, O. Rosier et al., Appl. Optics **65**, 5413 (1999).

[3] J. Pankert, K. Bergman, J. Klein et al., *in Proc. of SPIE* **4688**, 2002, p. 87–94.

[4] Yu.D. Korolev, O.B. Frants, V.G. Geyman et al., Rus. Fiz. Zh. **11**, Appendix, 217 (2006).

[5] Yu.D. Korolev, K. Frank, IEEE Trans. Plasma Sci. **27**, 1525 (1999).

[6] Lohte-Holtgrevena, ed., *The methods of plasma investigation*, Moscow, Mir, 1971.

[7] L.M. Biberman, V.S. Vorobjev, and I.I. Yakubov, Usp. Fiz. Nauk **128**, 233 (1979).